Selective Perhydroxylation of Squalene: Taming the Arithmetic Demon

Gerard A. Crispino, Pui Tong Ho, K. Barry Sharpless*

Osmium-catalyzed asymmetric dihydroxylation, which produces 1,2-diols of high enantiopurity from prochiral olefins, is an example of the synthetic catalysts that have been developed that rival enzymes in their efficiency and high enantioselectivity. Although the asymmetric dihydroxylation catalyst lacks an enzyme's ability to effectively distinguish among the subtly different olefinic sites in a polyolefin such as squalene, this very inability permits it to bring about the "exhaustive" polyhydroxylation of squalene to give a dodecahydroxy derivative. Twelve chemical and stereochemical events proceed in tandem with a remarkable average yield of 98 percent per step, giving 1 out of the 36 possible stereoisomers in $(0.98)^{12}$ = 78.9 percent overall yield.

Synthetic asymmetric catalysts are now available, some of which rival the enantioselectivities that enzymes have long been thought to monopolize (*1*). However, unlike enzymes, these synthetic asymmetric catalysts are made in both right- and left-handed forms, and in addition they often accept a wide range of substrates. Such distinctly nonenzymic generality makes these catalysts especially valuable for organic synthesis.

The osmium-catalyzed asymmetric dihydroxylation (AD) of olefins exhibits all of these desirable features: (i) high enantiomeric excess (ee) (*2*); (ii) substrate promiscuity; and (iii) a catalyst that is available in either enantiomeric form. Recent modifications boost the usefulness of AD for preparing optically active diols. Stirring a solution of the olefin with a premade mix, consisting of a catalytic amount of an osmium salt, a derivative (*3*) of the cinchona alkaloids dihydroquinidine or dihydroquinine 1 and 2 (*4*) (Fig. 1), and a cooxidant, gives the diol in excellent yield and ee.

For example, the catalytic AD of *trans*-stilbene shown in scheme 1 exhibits one of the highest ee's reported for a nonenzymic catalyst (*5*). By using the dihydroquinidine-based ligand, the *R,R* diol is formed in 99.8% ee (*6*).

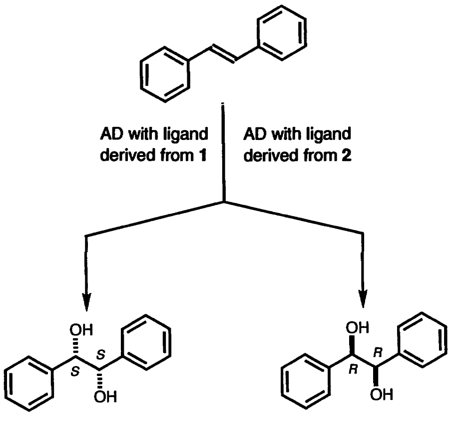

Scheme 1

The high enantioselectivity of ADs is not limited to simple olefins. Squalene is a triterpene and a hexaene that contains three kinds of trisubstituted double bonds in environments with slightly different degrees of steric hindrance. The ability to distinguish among these double bonds is an achievement for any catalyst, yet squalene monooxygenase, a key enzyme in the sterol biosynthesis pathway, deposits only a single oxygen atom on the squalene molecule and, by so doing, further chooses only the *si*-enantioface of the terminal double bond. In what is the closest nonenzymic mimic of this oxygenase, we recently reported that the AD catalyst described above also achieves regioselective dihydroxylation of the squalene terminal double bond in 96% ee (*7*). In contrast to the enzymic oxidation, the regioselectivity is only partial and the two internal diols, as well as various tetrols, also form. It is the inability of the chiral osmium catalyst to discriminate between the numerous trisubstituted alkene moieties in squalene that enable the AD process to effect the "exhaustive" AD of squalene (Fig. 2). Its high efficiency allows this process to overcome the "arithmetic demon," the precipitous drop in overall yield generally incurred by a long sequence of chemical reactions (*8*).

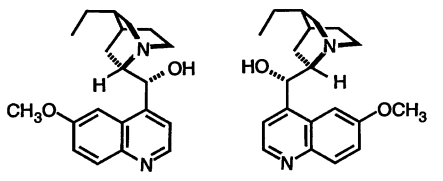

Dihydroquinine (DHQ) 1 Dihydroquinidine (DHQD) 2

Fig. 1. Cinchona alkaloids used in the AD.

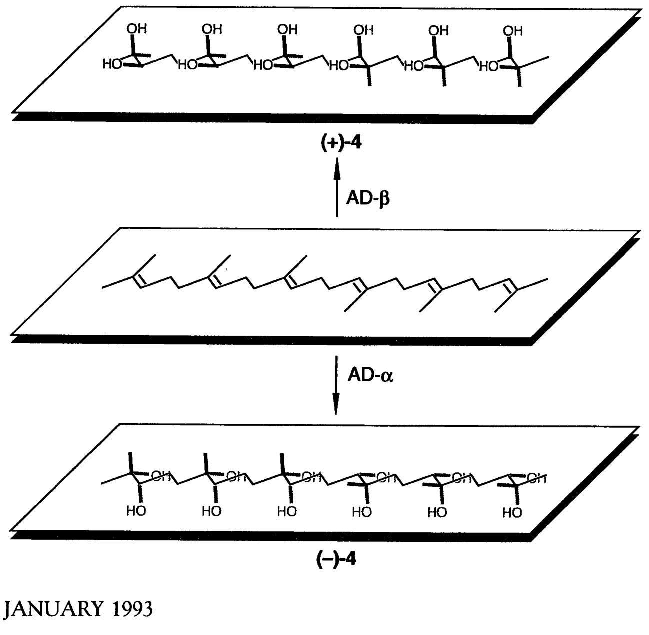

Fig. 2. The AD of squalene in which the dihydroquinidine-based ligand (AD-β) and the dihydroquinine-based ligand (AD-α) are used.

To ensure that the AD occurred in the organic phase, these exhaustive ADs were run in three stages and with acetonide formation after each run so that the hexaacetonides (+)-3 and (−)-3 were first isolated. Surprisingly, ^{1}H nuclear magnetic resonance (NMR) spectra revealed that each crude hexaacetonide product appeared to be a single isomer. A ^{14}C isotope dilution experiment (9) revealed that the crude fraction (88.3% yield) contained 89.3% of the desired product and that the remaining 10.7% was probably a mixture of some or all of the 35 other possible isomers. The pure compound was prepared from this crude material by recrystallization from cold pentane (*10*). The dihydroquinine-derived ligand gave a hexaacetonide with a rotation of −18.5°, whereas the dihydroquinidine-derived ligand gave a product with the opposite rotation of +18.1°. Because the dihydroquinidine ligand gives the *R* enantiomer in the AD of the 2,3-olefinic bond of squalene (*7*), we

---

Department of Chemistry, Scripps Research Institute, La Jolla, CA 92037.

*To whom correspondence should be addressed.

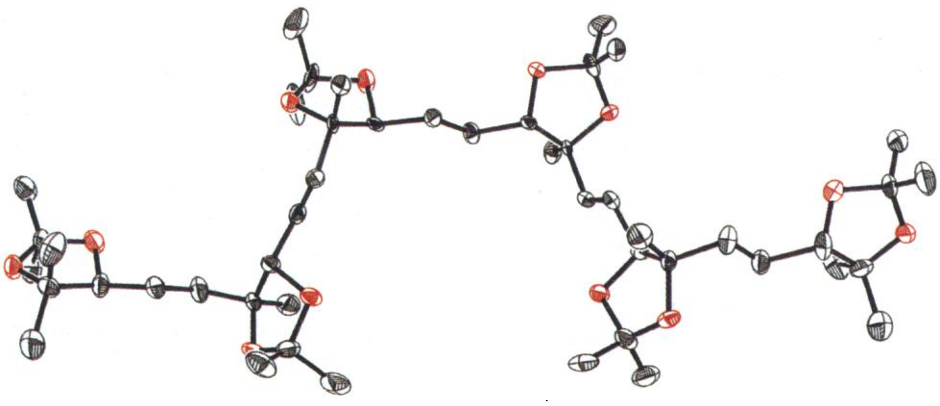

Fig. 3. X-ray crystal structure of squalene dodecaol hexaacetonide (−)-**3**.

assign the (+)-hexaacetonide the all-*R* configuration and the (−)-hexaacetonide the all-*S* configuration. The expected structure of the hexaacetonides was confirmed by the x-ray structure of (−)-3 (Fig. 3).

The selectivities and yields implied for each of the six sequential oxidations required in Fig. 2 are gratifyingly high. Of the 64 possible stereoisomers, 28 are removed by symmetry to give 36 unique products: 12 pairs of unsymmetrical isomers, 4 pairs with C_2 symmetry, and 4 *meso*-compounds (Fig. 4) (*11*). In the absence of ligand, only a statistical amount of racemic (±)-3 is expected, that is, 2/64 or 3.13%. The use of the isotope dilution technique (*12*) showed that the crude mixture contained 4.38% of (±)-3 when the osmylation was performed without ligand. In contrast, when the ligand is used, the labeling results described above give an overall yield of 78.9% of enantiomerically pure (+)-3 (based on an 88.3% isolated yield of 89.3% pure crude product) for the six reactions (one that is enantioselective and five that are diastereoselective). This yield requires that each of the six AD events must proceed in 98% ee or diastereomeric excess and 98% yield on average because $(78.9\%)^{1/12}$ = 98% (*13*).

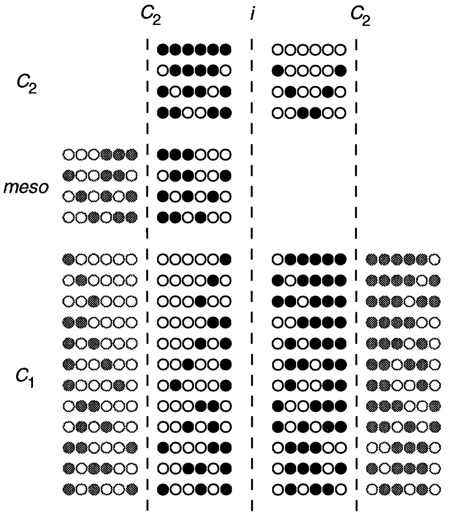

Fig. 4. The relation of the 64 (2^6) isomers. The symmetry operations listed at the top reduce the number of isomers to 36: 4 C_2 symmetrical diastereomers and their enantiomers, 4 *meso* diastereomers that have no enantiomers, and 12 diastereomers with no symmetry and their enantiomers. Each circle may be thought of as a disk that is white on one side and black on the other. The C_2 operation is a twofold rotation axis normal to the plane of the page between the third and fourth circles. The *i* operator is an inversion center (center of symmetry) between the third and fourth circles. The 28 gray representations in the two outside columns are the isomers removed by symmetry considerations.

The hexaacetonide enantiomers are easily converted to the corresponding dodecaols (+)-4 and (−)-4 by treatment with aqueous hydrochloric acid in acetonitrile (*14*). Unlike the acetonides, the dodecaols are highly insoluble in organic solvents. They have very slight solubility in cold water but dissolve irreversibly in hot water. The chemical structure of the dissolved material remains unchanged (as determined by the ^{1}H NMR spectrum in D_2O), which may suggest that the dodecaols have a secondary structure that results from the many possible intramolecular hydrogen bonds.

The high yield of a single enantiomer from the multiple hydroxylation events required to completely oxidize squalene reflects the reliability and selectivity of the AD process and demonstrates the progress being made in selective abiological catalysis.

REFERENCES AND NOTES

1. J. D. Morrison, Ed., *Asymmetric Synthesis* (Academic Press, Orlando, FL, 1985), vol. 5.
2. Enantiomeric excess (ee) is defined as the percent difference between the major and minor enantiomers.
3. Our best ligand to date contains two of the cinchona alkaloid units connected by a 1,4-phthalazine spacer: K. B. Sharpless *et al.*, *J. Org. Chem.* **57**, 2768 (1992).
4. Dihydroquinidine and dihydroquinine are actually diastereomers in that they have opposite chirality at only four of the five stereogenic centers (the ethyl-bearing carbons have identical configurations). However, the alkaloids behave like enantiomers because each gives a product of opposite chirality.
5. For an example of high enantioselectivity in the asymmetric hydrogenation of acetamidoacrylates, see M. J. Burk, *J. Am. Chem. Soc.* **113**, 8518 (1991).
6. None of the *S,S* enantiomers could be detected when the reaction product was analyzed by high-performance liquid chromatography. Only when the product was recrystallized from 95% ethanol could the minor isomer be detected in the mother liquor.
7. G. A. Crispino and K. B. Sharpless, *Tetrahedron Lett.* **33**, 4273 (1992).
8. For example, a synthetic sequence involving 12 linear steps, each occurring in 90% yield, will only give $(0.9)^{12}$ = 28% overall yield. See R. E. Ireland, *Organic Synthesis* (Prentice-Hall, Englewood Cliffs, NJ, 1969).
9. This isotope dilution experiment was performed as follows: A sample of **3** was labeled with ^{14}C acetone, and the product was purified to constant radioactivity by repeated recrystallization. A known quantity of this material was mixed with a known amount of the chromatographed product from the serial dihydroxylation/acetonide protection procedure, and this mixture was purified to constant activity by repeated recrystallization. The dilution in the label corresponds to the amount of **3** in the chromatographed sample.
10. The hexaacetonides (+)-**3** and (−)-**3** have the following spectral data. ^{1}H NMR ($CDCl_3$, 400 MHz): δ 3.79 (d, *J* = 9.0 Hz, 1 H), 3.70 (dd, *J* = 8.6 Hz, *J′* = 3.1 Hz, 1 H), 3.62 (dd, *J* = 8.8 Hz, *J′* = 3.6 Hz, 1 H), 1.78 to 1.47 (m, 10 H), 1.42 (s, 3 H), 1.41 (s, 3 H), 1.40 (s, 3 H), 1.32 (s, 3 H), 1.31 (s, 6 H), 1.23 (s, 3 H), 1.103 (s, 3 H), 1.100 (s, 3 H), and 1.09 (s, 3 H). ^{13}C NMR ($CDCl_3$, 100 MHz): δ 106.62, 106.45, 83.79, 81.79, 81.76, 81.73, 80.46, 80.06, 35.84, 35.70, 28.65, 28.60, 28.47, 26.82, 26.53, 26.12, 23.69, 23.55, 22.92, 21.98, and 21.85. High-resolution mass spectrum: calculated for $C_{48}H_{86}O_{12}$ (M + Cs^+), 987.5174; found, 987.5144. Combustion analysis: calculated for $C_{48}H_{86}O_{12}$, C, 67.41, and H, 10.14; found, C, 67.21, and H, 9.85. Melting point: 111° to 112°C.
11. Although squalene dodecaol has 12 hydroxylated sites, of which 10 are stereogenic centers, the problem of the number of isomers is considerably reduced because all of the hydroxyls arise from *syn* addition to only six olefins. Hence, instead of considering 2^{10} (1024) possible isomers, we need consider only 2^6 (64). The symmetry of squalene (C_{2h} or C_{2v}) further reduces the number of possible isomers. In general for problems of this symmetry, it can be shown that for a molecule with *n* independent sites:
   For *n* even:
   The number of *meso* diastereomers equals the number of C_2 diastereomers and is $2^{(n/2-1)}$. The number of unsymmetrical diastereomers is $2^{(n-2)} - 2^{(n/2-1)}$.
   For *n* odd:
   There are no C_2 symmetrical isomers for *n* odd. The number of *meso* diastereomers is $2^{(n-1)/2}$. The number of unsymmetrical diastereomers is $2^{(n-2)} - 2^{(n-3)/2}$.
   The results are that there are 4 *meso* diastereomers, 4 C_2 diastereomers (and their enantiomers), and 12 unsymmetrical diastereomers (and their enantiomers) for a total of 36 isomers.
12. This isotope dilution was performed as follows: The serial dihydroxylation/acetonide protection procedure was performed in the absence of the ligand, and the resulting mixture of acetonides purified chromatographically. This mixture was labeled with ^{14}C acetone and then chromatographed. A known quantity of this product was mixed with a known quantity of (+)-**3**, and the resulting mixture was purified to constant activity by repeated recrystallization. The amount of (±)-**3**

in the mixture of acetonides can be calculated by comparison of the activity of the recrystallized product with the activity of the labeled mixture of acetonides.

13. Like the yield dependence of the six linear steps (*8*), the six tandem stereoselective events are also linearly related. For earlier discussions of this latter phenomenon, see J. P. Vigneron, M. Dhaenens, A. Horeau, *Tetrahedron* **29**, 1055 (1973); T. R. Hoye and J. C. Suhadolnik, *ibid.* **42**, 2855 (1986); S. L. Schreiber, T. S. Schreiber, D. B. Smith, *J. Am. Chem. Soc.* **109**, 1525 (1987); V. Rautenstrauch, P. Mégard, B. Bourdin, A. Furrer, *ibid.* **114**, 1418 (1992).
14. The dodecaols (+)-**4** and (−)-**4** have the following spectral data. ^{1}H NMR (D_2O, 400 MHz): δ 3.33 (d, $J = 10.4$ Hz, 1 H), 3.23 (d, $J = 10.2$ Hz, 1 H), 3.15 (d, $J = 10.4$ Hz, 1 H), 1.65 to 1.37 (m, 8 H), 1.24 to 1.15 (m, 2 H), 1.02 (s, 6 H), 0.993 (s, 3 H), and 0.991 (s, 3 H). ^{13}C NMR (dimethyl sulfoxide-d_6, 100 MHz): δ 78.41, 77.92, 77.02, 73.55, 73.49, 71.75, 35.16, 35.03, 28.27, 26.27, 24.74, 24.65, 22.69, and 22.59. High-resolution mass spectrum: calculated for $C_{30}H_{62}O_{12}$ (M + Na$^+$), 637.4139; found, 637.4139. Combustion analysis: calculated for $C_{30}H_{62}O_{12}\cdot H_2O$, C, 56.94, and H, 10.19; found C, 56.59, and H, 10.00. Melting point: 195° to 198°C (decomposes). Optical rotations: $[\alpha]_D^{24\,5}$ + 53.6° ($c = 0.5$, H_2O) for (+)-**4**, $[\alpha]_D^{22\,5}$ − 49.0° ($c = 0.5$, H_2O) for (−)-**4**.
15. Financial support was provided by the National Institutes of Health (GM 28384) and the National Science Foundation (CHE-8903218). We thank R. Chadra for providing the x-ray crystal structure of the hexaacetonide (−)-**3** and D. Rideout for his assistance with the ^{14}C isotope dilution experiments.

15 September 1992; accepted 9 November 1992

Effect of Pressure on the Composition of the Lower Mantle End Member Fe_xO

Catherine McCammon

The composition limits of Fe_xO are sensitive to both pressure and temperature. Earlier studies have shown that Fe_xO becomes highly nonstoichiometric when in equilibrium with metallic iron above 10 gigapascals, which is difficult to reconcile with available thermodynamic data. Experiments with a uniaxial split-sphere apparatus demonstrate that the iron content of Fe_xO increases continuously at high pressure in excellent agreement with quantitative models and suggest that there is a discontinuity in the elastic properties of Fe_xO above $x = 0.95$. On the basis of these results, it is inferred that the Earth's present lower mantle is not in equilibrium with metallic iron.

Knowledge of the amount of Fe^{3+} in Fe_xO, and ultimately in (Mg,Fe)O, is of fundamental importance to studies of lower mantle properties such as electrical conductivity and oxygen fugacity (f_{O_2}). The maximum Fe content of Fe_xO at atmospheric pressure is limited to about $x = 0.95$, which corresponds to $Fe^{3+}/\Sigma Fe = 0.11$ on the basis of electrostatic charge balance. Although studies have shown that more stoichiometric samples can be synthesized at pressures up to 10 GPa (*1*–*4*), experiments at higher pressures indicate that Fe_xO becomes significantly less stoichiometric in equilibrium with metallic Fe (*4*, *5*) (Fig. 1). Although such behavior can be understood qualitatively in terms of a composition-dependent bulk modulus for Fe_xO, the extreme nonstoichiometry along the Fe-Fe_xO phase boundary at higher pressures cannot be explained (*4*). Small sample sizes have caused large uncertainties in earlier determinations of Fe-Fe_xO phase relations, but recent advances in high-pressure technology allow the recovery of several milligrams of sample. The wide pressure range available enables all experiments to be performed on one type of apparatus, which avoids inconsistencies resulting from different f_{O_2} conditions. In this study, I used a multianvil press to determine accurately the Fe-Fe_xO phase boundary at high pressure and temperature.

As described in (*4*), $Fe_{0.952}O$ was prepared at atmospheric pressure in an evacuated silica glass tube, mixed with Fe powder in the molar ratio 10:1, and packed into an Fe capsule to buffer f_{O_2} conditions during the run. I performed the experiments on a 1200-T split-sphere multianvil apparatus with the use of Cr_2O_3-doped MgO octahedra as a pressure medium. In runs up to 10 GPa, I used 18-mm (edge) octahedra with a stepped graphite heater (*6*), whereas for runs from 14 to 18 GPa, I used 10-mm (edge) octahedra with a $LaCrO_3$ heater. Each run lasted 1 hour (*7*). Pressure was calibrated at room temperature with the use of transitions in Bi, ZnS, and GaS; at 1000°C with quartz-coesite and coesite-stishovite reactions (18-mm assembly); and at 1200° and 1600°C with the olivine–β-phase and β-phase–spinel transitions in Mg_2SiO_4 (10-mm assembly). Temperatures were initially measured with a $W_{75}Re_{25}$-$W_{97}Re_3$ thermocouple but, because of thermocouple failure during the compression phase of each experiment, I estimated the final temperature on the basis of a calibrated power curve derived from a minimum of three previous experiments that were carried out on the same assembly at the same pressure and temperature conditions. I performed one additional experiment on a conventional piston cylinder press. The final composition of each sample was determined by x-ray diffraction on the basis of the linear relation between cubic cell parameter and iron composition (*4*). Mössbauer spectra were recorded at both room temperature and 80 K to correlate hyperfine parameters with expected Fe^{3+} content (*8*). The Mössbauer parameters were consistent with the composition determined by x-ray diffraction.

The results of all runs (Table 1) indicate that the Fe content of Fe_xO in equilibrium with metallic Fe increases with pressure until reaching a plateau near $Fe_{0.98}O$. There is clearly no decrease in Fe content above 10 GPa as previously observed. Although a change in composition during the quenching process cannot be completely ruled out, the observation that the limiting composition ($Fe_{0.98}O$) was the same as earlier experimental results at 775°C (*1*) argues against such a possibility. A temperature uncertainty of ±100°C is estimated to contribute a maximum uncertainty of ±0.001 in x (*9*).

One explanation for the extremely low Fe content obtained in the earlier experiments is that Fe_xO is difficult to heat in diamond-anvil cell experiments because it absorbs laser radiation poorly at high pressure (*4*); thus, temperatures may have been overestimated. The γ-ε transition in Fe occurs near 780°C at 20 GPa (*10*), and temperatures lower than this boundary

Table 1. Details of high-pressure runs on Fe_xO in equilibrium with metallic Fe. Uncertainties are given in parentheses.

Synthesis technique	Pressure (GPa)	Temperature (°C)	Cell dimension (a) of Fe_xO (pm)	Fe_xO composition*
Evac. silica tube		1000(5)	431.09(5)	0.952(2)
Piston cylinder	1.5(5)	1000(10)	431.35(5)	0.957(2)
Multianvil press	5.0(5)	1000(50)	431.92(5)	0.969(2)
Multianvil press	10.0(5)	1000(100)	432.37(5)	0.978(2)
Multianvil press	14.0(5)	1000(100)	432.41(5)	0.979(3)
Multianvil press	18.0(5)	1000(100)	432.44(5)	0.980(2)

*Calculated from $a = 385.6 + 47.8x$ (*4*).

Bayerisches Geoinstitut, Postfach 10 12 51, W-8580 Bayreuth, Germany.